31st Annual International Conference of the IEEE EMBS
Minneapolis, Minnesota, USA, September 2-6, 2009

An Anatomical Mouse Model for Multimodal Molecular Imaging

Xing Zhang, Jie Tian*, *Senior member, IEEE,* Jinchao Feng, Shouping Zhu and Guorui Yan

***Abstract*— In order to evaluate and improve multimodal molecular imaging technology, a three-dimensional anatomical model of a BALB/c mouse was developed based on micro-CT imaging with a liver-specific contrast agent Fenestra LC. By using image processing and interactive segmentation methods, we delineated some primary organs and tissues, including the skin, skeleton, muscle, heart, lung, liver and spleen. Finally, cone-beam x-ray CT and bioluminescence tomography simulation experiments demonstrate the availability and flexibility of the proposed mouse model.**

I. INTRODUCTION

Molecular imaging is a refined and promising technology aimed at non-invasive, quantitative visualization of *in vivo* molecular processes occurring at cellular levels [1]. The rapid development in multimodal molecular imaging with combination of optical imaging and x-ray CT has stimulated interest in models of small animals, which have comprehensive applications in both simulation and *in vivo* imaging. As an emerging and promising biomedical imaging field, molecular imaging is involved with integration of imaging devices and reconstruction technologies to study biological and medical processes. Meanwhile, how to evaluate and improve the performance of these techniques is a challenge currently confronted by multimodal molecular imaging. Computational models of both the anatomy and physiological functions of small animals provide an accurate and realistic simulation tool for biomedical imaging that are ever closer to those obtained from experimental small animal studies.

As the most widely used experimental animals, mouse and rat have significant influence on genetics, pathology, pharmacology and gene expression studies. In recent years, much research has been done on computational mouse models. The current mouse models can be classified into two categories according to the modalities from which they were constructed: serial cryosection data and magnetic resonance microscopy (MRM/μMRI) data. The former include the 3D whole body mouse atlas created from coregistered micro-CT and cryosection data developed by the University of Southern California [2] and the Sprague-Dawley rat model from the Britton Chance Center for Biomedical Photonics [3], the latter include the 4D MOBY phantom [4] using the MRM dataset obtained from the Duke Center for *In Vivo* Microscopy, the Caltech μMRI atlas of mouse development [5], the EMAP Edinburgh spatio-temporal mouse atlas project for gene expression studies [6] and the 3D MRM digital atlas database of an adult C57BL/6J mouse brain at the Brookhaven National Laboratory [7].

In this paper, studies were performed on a BALB/c mouse, one of the most widely used inbred strains used in animal experimentation. An independently developed micro-CT imaging system [8] along with a reconstruction software of FDK filtered backprojection method using GPU hardware [9] was applied in construction of the mouse model. Compared with the computational mouse models listed above, we obtained the model of primary organs and tissues from non-invasive micro-CT imaging with injection of a contrast agent for multimodal molecular imaging. Furthermore, availability of the model has been proved through cone-beam x-ray CT and bioluminescence tomography simulation experiments. In addition to promoting the development of imaging equipments and reconstruction methods across modalities, the anatomical structure of real mouse can be applied to radiation dosimetry calculations and external radiation therapy with a *priori* knowledge of radiation sources and distribution.

II. MATERIALS AND METHODS

A. Mouse preparation

All animal studies were conducted under protocols approved by the Animal Care and Use Committee. BALB/c is an albino strain of laboratory mouse which has extensive applications in cancer, immunology and monoclonal antibody production. We chose it for convenient tail vein injection in albino mouse and broad applications in biological and medical research.

ART's Fenestra LC is an iodinated lipid emulsion blood-pool contrast agent that provides visualization of the hepatobiliary system during micro-CT scans of mice and other small animals to help overcome the problem of inherently soft tissue contrast in micro-CT imaging. Fenestra technology improves the quality of the *in vivo* imaging and enables researchers to perform multifarious studies.

We prepared a 20 g male BALB/c mouse for our study. After fasting for 24 hours, the mouse tail was immersed in warm water for 30-60 seconds to increase blood flow to the tail and dilate the vessels prior to injection of the contrast agent. Restraining the mouse in a test tube, the Fenestra LC at a dose of 15 mL/kg was slowly injected over a period of 30-60 seconds via the lateral tail vein. The mouse was then anesthetized with intraperitoneal injection of a 15% aqueous urethane (0.15 mL/20 g body weight).

This work is supported by NBRPC (2006CB705700), PCSIRT (IRT0645), CAS SREDP (YZ0642, YZ200766), JRFOCYS (30528027), NSFC (30672690, 30600151, 60532050, 60621001, 30873462), BNSF (4071003), TKPBEC (KZ200910005005) in China.

Xing Zhang, Jie Tian, Jinchao Feng, Shouping Zhu and Guorui Yan are with Medical Image Processing Group, Institute of Automation, Chinese Academy of Sciences. e-mail: tian@ieee.org

B. Micro-CT imaging

The first scanning was performed [8] 40 minutes after injection of the contrast agent. The mouse was immobilized head downward on a polymethyl methacrylate (PMMA) panel mouseholder. During scanning, the x-ray source is operated in a continuous mode with a 1 mm aluminum filter, and the typical tube voltage is 50 KVp. X-ray settings included tube current 1.4 mA and integrated time 0.6 s. The source to detector distance (SDD) and source to object distance (SOD) were set to 541.36 mm and 448.50 mm, respectively, and the magnification ratio is 1.2. After 15 minutes scanning, 500 projection views with image size of 2240×2344 pixels and pixel size 0.05×0.05 mm were obtained by 360^o full scan in 0.72^o steps.

Micro-CT scanning was also performed for comparison following the first scanning protocols at 3.5 hour after contrast. As shown in Fig. 1, peak was reached at 3.5 hour post-injection for imaging purposes in accordance with the user guide of Fenestra LC. The 3.5 hour post-injection imaging data were reconstructed for model generation.

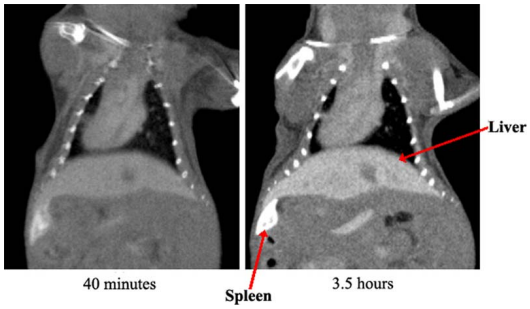

Fig. 1. A comparison of coronal images of the mouse imaging at 40 min and 3.5 h post-injection of Fenestra LC.

The FDK filtered backprojection method using GPU hardware [9] was applied in 3D reconstruction. 2×2 binning was performed on projection views before reconstruction to increase signal-noise ratio (SNR). Finally, the mouse volume data were reconstructed from 500 projection views of the image size 1120×1172 pixels at the resolution 0.1×0.1 mm, and the reconstructed volume data acquired as transverse sections were cropped to $384 \times 600 \times 960$ ($coronal \times sagittal \times transverse$) with an isotropic voxel size of 0.1 mm.

C. Segmentation

After micro-CT imaging and 3D reconstruction, we imported the volume data into our 3DMed (http://www.3dmed.net/, http://www.mitk.net/) software [10] which integrates the basic functions of data input/output, segmentation, registration, 3D visualization and measurement. The volume data of the mouse can be viewed in three orthogonal planes (transverse, coronal and sagittal) or in any arbitrary oblique plane. We then adjusted window width and level of the image to obtain the best display of soft tissue.

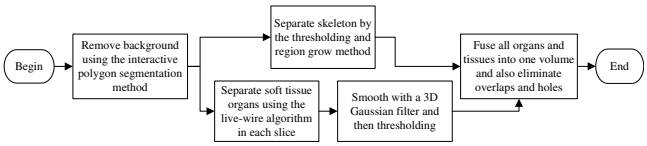

Fig. 2. The flow chart of the segmentation process.

The segmentation process was conducted under the flow chart shown in Fig. 2. First we removed the background by using the interactive polygon segmentation method in transverse sections. The skeleton was then separated for the highest CT value (more than 1000 HU) via combination of the threshold and region grow algorithms. In order to delineate several soft tissue structures, including the heart, lung, liver and spleen, we applied some interactive and manual segmentation methods in consecutive sections. For instance, as the lung structure has distinct contour with neighboring organs caused by its low CT value, an intelligent scissors (live wire) segmentation method was applied to trace the boundary in consecutive transverse sections. The segmentation result of lung was then refined in the other two coronal and sagittal sections. The same measure was taken for separation of liver in coronal sections considering the high contrast resulted from the contrast agent Fenestra LC. As for thoracoabdominal organ volumes, smoothing is a indispensable step that can be implemented by convolution with a 3D Gaussian filter and then thresholding with the median value. In the meantime to fuse the separated organ and tissue volumes, we eliminated overlaps and holes via the ITK-SNAP tool by manual delineating. Fig. 3 shows the original micro-CT data and the labeling of organs and tissues in the coronal and transverse planes.

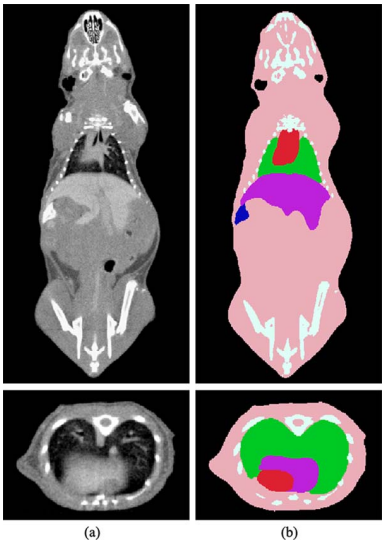

Fig. 3. (a) Coronal and transverse images of micro-CT data; (b) Labeling of organs and tissues in the coronal and transverse planes.

Visualization of the final fused volume of various organs and tissues was performed by surface rendering using the marching cubes algorithm in the same view. Surface render-

ing of the separated organs and tissues is presented in Fig. 4.

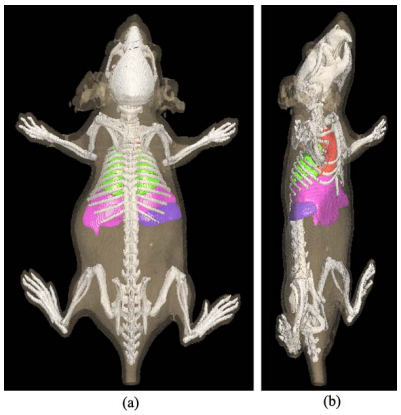

Fig. 4. Surface rendering of the separated organs and tissues: skin, skeleton, heart, lung, liver, spleen. (a) Dorsal-ventral view; (b) Left lateral view.

The original micro-CT imaging and the anatomical model data are available at the website http://www.mosetm.net/. All data are provided in Meta format containing an ASCII readable header and a separate raw image data file. This format is ITK compatible.

III. EXPERIMENTS AND RESULTS

There are several potential applications for our mouse model such as simulation of x-ray CT, MRI, PET and bioluminescence tomography imaging systems. The realistic model based on anatomy of mouse contributes to improvement of imaging equipments and reconstruction methods across modalities, *e.g.* simulation results provide information to optimize algorithms and systems.

To illustrate applications of the model, cone-beam x-ray CT and bioluminescence tomography simulation experiments were performed respectively.

A. Cone-beam x-ray CT simulation

Cone-beam x-ray CT simulation based on the anatomical model is generally involved in projection simulation and image reconstruction algorithm. In the computation of projection simulation for voxel model traverse along 3D ray beam, the same parameters as the above micro-CT imaging were set for comparison. We developed a FDK filtered backprojection algorithm using GPU hardware to accelerate reconstruction [9]. The computation time of reconstructing a 512 cubed volume from 360 views of the image size of 512×512 is about 5.2 s on a 2.66 GHz dual-core Intel PC with 2 GB RAM hosting a Nvidia Geforce 8800GTX card.

To simulate realistic noise conditions, a total of 500 projection views were simulated and the projection image data were obtained by adding Gaussian noise to the numerical computed projections. Fig. 5(a) shows transverse images of cone-beam x-ray CT simulation using the mouse atlas, which are compared with images acquired from a live mouse, as shown in Fig. 5(b). Potential applications in CT simulation include image quality and reconstruction algorithms evaluation.

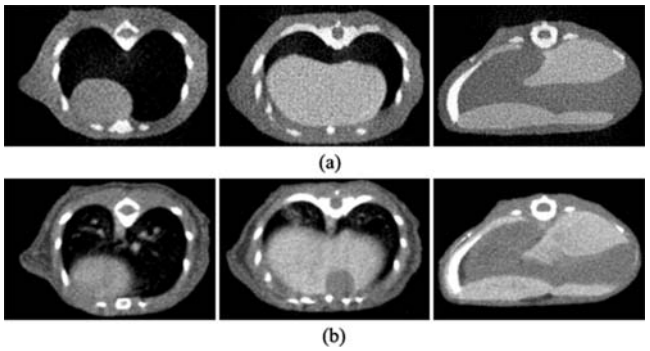

Fig. 5. (a) Transverse images of cone-beam x-ray CT simulation using the mouse model; (b) Transverse images acquired from the live mouse using micro-CT imaging system.

TABLE I

OPTICAL PARAMETERS OF THE REAL MOUSE [11]

Material	Muscle	Lung	Heart	Bone	Liver
$\mu_a[mm^{-1}]$	0.01	0.35	0.2	0.002	0.3
$\mu_s[mm^{-1}]$	4.0	23.0	16.0	20.0	6.0
g	0.9	0.94	0.85	0.9	0.9

B. Bioluminescence tomography simulation

Since the anatomical structure of a real mouse greatly reduces the ill-posedness of bioluminescence tomography (BLT), the scanned anatomical information is significant to BLT reconstruction. In bioluminescence experiment, the thorax micro-CT images were used after the real mouse was segmented into different tissue organs, including the lung, bone, heart, liver and muscle, shown in Fig. 6(a). Optical parameters from the literature [11] and the references therein were assigned to each of the five components, as listed in Table. I. For BLT reconstruction, the mouse was discretized into a tetrahedral-element mesh, as shown in Fig. 6(b).

It's well known that bioluminescence tomography is an inverse problem. Therefore, the inverse crime is likely to occur when closely correlated computational ingredients are used in the forward solver and the inverse scheme. In order to avoid the inverse crime, the synthetic data were produced by a Molecular Optical Simulation Environment (MOSE) based on Monte Carlo method, which may employ the micro-CT/MRI slices to define the object geometry [12]. The mesh used in MOSE was demonstrated in Fig. 6(c).

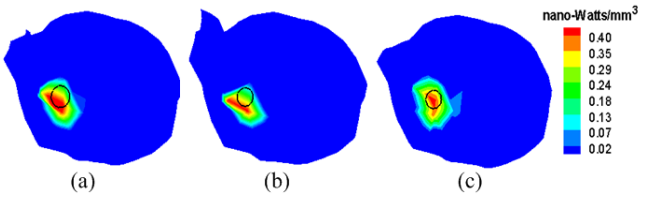

Fig. 7. Reconstruction results. (a) The transverse section perpendicular to z-axis direction is through the actual source's center; (b) and (c) are ± mm off the actual source's center. The black circle denotes the actual source positions.

In bioluminescence imaging, a solid spherical source

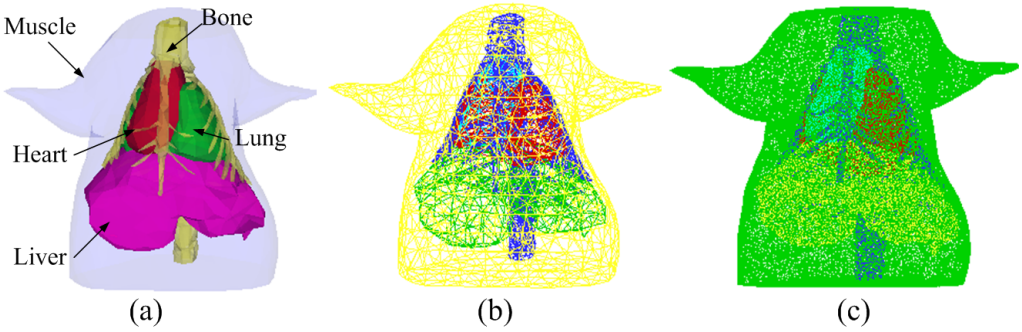

Fig. 6. (a) Heterogeneous phantom with Muscle, Bone, Heart, Liver and Lung; (b) The initial mesh used in the tomographic algorithm; (c) The discretized mesh of the phantom used in MOSE.

with 1mm radius was centered at $(22.3, 28.1, 12.5)$(unit:mm) inside the lung. With the method proposed in [13], the reconstructed results were demonstrated in Fig. 7. Fig. 7 reveals that the source can be preferable localized.

IV. CONCLUSIONS AND FUTURE WORKS

Molecular imaging techniques aim to characterize and quantify physiological and pathological processes *in vivo* at the cellular and molecular levels. With combination of multimodality (*e.g.* optical imaging and x-ray CT), pathophysiological changes in early disease phases at high structural resolution can be detected. Small animal models play an important role in demonstration and appraisal of imaging equipments and reconstruction algorithms. In this paper, we have presented a three-dimensional voxel-based model of a BALB/c mouse based on micro-CT imaging with Fenestra liver-specific contrast agent (LC). The original micro-CT imaging and the anatomical model data for free download are available at the website http://www.mosetm.net/. Cone-beam x-ray CT and bioluminescence tomography simulation experiments were performed to demonstrate the availability and flexibility of the proposed mouse model.

In future work, we will concentrate on constructing the whole body mouse model of both the anatomy and physiological functions across modalities of micro-CT, cryosection and magnetic resonance microscopy. The mouse model will extensively promote our multimodal molecular imaging. Furthermore, comprehensive potential applications of the mouse model will be explored, *e.g.*, PET simulation, radiation dosimetry calculations and external radiation therapy.

REFERENCES

[1] J. Tian, J. Bai, X. Yan, S. Bao, Y. Li, W. Liang and X. Yang, "Multimodality Molecular Imaging", *IEEE Eng. Med. Biol. Mag.* vol. 27, 2008, pp 48-57.

[2] B. Dogdas, D. Stout, A. F. Chatziioannou and R. M. Leahy, "Digimouse: a 3D whole body mouse atlas from CT and cryosection data", *Phys. Med. Biol.* vol. 52, 2007, pp 577-588.

[3] L. Wu, G. Zhang, Q. Luo and Q. Liu, "An image-based rat model for Monte Carlo organ dose calculations", *Med. Phys.* vol. 35, 2008, pp 3759-3764.

[4] W. P. Segars, B. M. W. Tsui, E. C. Frey, G. A. Johnson and S. S. Berr, "Development of a 4D Digital Mouse Phantom for Molecular Imaging Research", *Mol. Imaging. Biol.* vol. 6, 2004, pp 149-159.

[5] M. P. Dhenain, S. W. Ruffins and R. E. Jacobs, "Three-Dimensional Digital Mouse Atlas Using High-Resolution MRI", *Dev. Biol.* vol. 232, 2001, pp 458-470.

[6] R. A. Baldock, J. B. L. Bard, A. Burger, N. Burton, J. Christiansen, G. Feng, B. Hill, D. Houghton, M. Kaufman and J. Rao, "EMAP and EMAGE: A Framework for Understanding Spatially Organized Data", *Neuroinformatics* vol. 1, 2003, pp 309-325.

[7] Y. Ma, P. R. Hof, S. C. Grant, S. J. Blackband, R. Bennett, L. Slatest, M. D. McGuigan and H. Benveniste, "A three-dimensional digital atlas database of the adult C57BL/6J mouse brain by magnetic resonance microscopy", *Neuroscience* vol. 135, 2005, pp 1203-1215.

[8] S. Zhu, J. Tian, G. Yan, C. Qin and J. Liu, "An experimental cone-beam micro-CT system for small animal imaging", *SPIE Medical Imaging* vol. 7258, 2009, pp 72582S-1-10.

[9] G. Yan, J. Tian, S. Zhu, Y. Dai, and C. Qin, "Fast cone-beam CT image reconstruction using GPU hardware", *IJ. X-Ray Sci. Technol.* vol. 16, 2008, pp 225-234.

[10] J. Tian, J. Xue, Y. Dai, J Chen and J. Zheng, "A Novel Software Platform for Medical Image Processing and Analyzing", *IEEE T. Inf. Technol. Biomed.* vol. 12, 2008, pp 800-812.

[11] Y. Lv, J. Tian, W. Cong, G. Wang, J. Luo, W. Yang, and H. Li, "A multilevel adaptive finite element algorithm for bioluminescence tomography", *Opt. Express* vol. 14, 2006, pp 8211-8223.

[12] H. Li, J. Tian, F. Zhu, W. Cong, L. V. Wang, E. A. Hoffman, and G. Wang, "A mouse optical simulation environment (MOSE) to investigate bioluminescent phenomena in the living mouse with the Monte Carlo method", *Acad. Radiol.* vol. 11, 2004, pp 1029-1038.

[13] J. Feng, K. Jia, J. Tian, G. Yan, and C. Qin, "Bioluminescence tomography based on Bayesian approach", *SPIE Medical Imaging* vol. 7262, 2009, pp 72620R-1-8.